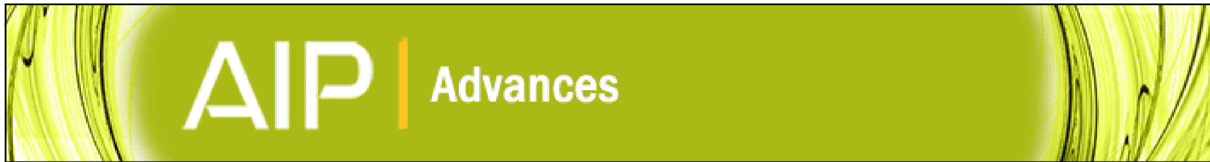

Tunable atomic force microscopy bias lithography on electron beam induced carbonaceous platforms

Narendra Kurra

Citation: AIP Advances **3**, 092108 (2013); doi: 10.1063/1.4821271
View online: http://dx.doi.org/10.1063/1.4821271
View Table of Contents: http://scitation.aip.org/content/aip/journal/adva/3/9?ver=pdfcov
Published by the AIP Publishing

Articles you may be interested in

The fabrication of nanomesas and nanometal contacts by using atomic force microscopy lithography
J. Appl. Phys. **108**, 094316 (2010); 10.1063/1.3504654

Atomic force microscope based nanofabrication of master pattern molds for use in soft lithography
Appl. Phys. Lett. **91**, 123111 (2007); 10.1063/1.2787965

Tribonanolithography of silicon in aqueous solution based on atomic force microscopy
Appl. Phys. Lett. **85**, 1766 (2004); 10.1063/1.1773620

Nanostructuring of silicon by electron-beam lithography of self-assembled hydroxybiphenyl monolayers
Appl. Phys. Lett. **82**, 3776 (2003); 10.1063/1.1578537

Fabrication of mesoscopic devices using atomic force macroscopic electric field induced oxidation
J. Vac. Sci. Technol. B **21**, 162 (2003); 10.1116/1.1537712

Goodfellow
metals • ceramics • polymers
composites • compounds • glasses
Save 5% • Buy online
70,000 products • Fast shipping

All article content, except where otherwise noted, is licensed under a Creative Commons Attribution 3.0 Unported license. See: http://creativecommons.org/licenses/by/3.0/
Downloaded to IP: 129.21.35.191 On: Sun, 21 Dec 2014 15:36:59

AIP ADVANCES 3, 092108 (2013)

Tunable atomic force microscopy bias lithography on electron beam induced carbonaceous platforms

Narendra Kurra[a]
Chemistry and Physics of Materials Unit, Jawaharlal Nehru Centre for Advanced Scientific Research, Jakkur PO, Bangalore 560 064, India

(Received 28 May 2013; accepted 26 August 2013; published online 10 September 2013)

Tunable local electrochemical and physical modifications on the carbonaceous platforms are achieved using Atomic force microscope (AFM) bias lithography. These carbonaceous platforms are produced on Si substrate by the technique called electron beam induced carbonaceous deposition (EBICD). EBICD is composed of functionalized carbon species, confirmed through X-ray photoelectron spectroscopy (XPS) analysis. AFM bias lithography in tapping mode with a positive tip bias resulted in the nucleation of attoliter water on the EBICD surface under moderate humidity conditions (45%). While the lithography in the contact mode with a negative tip bias caused the electrochemical modifications such as anodic oxidation and etching of the EBICD under moderate (45%) and higher (60%) humidity conditions respectively. Finally, reversible charge patterns are created on these EBICD surfaces under low (30%) humidity conditions and investigated by means of electrostatic force microscopy (EFM). © *2013 Author(s). All article content, except where otherwise noted, is licensed under a Creative Commons Attribution 3.0 Unported License.* [http://dx.doi.org/10.1063/1.4821271]

I. INTRODUCTION

Atomic force microscopy (AFM) is a powerful characterization tool for imaging the surface morphology with atomic and molecular resolution.[1] As AFM relies on the local tip-sample forces, it has been employed to study a variety of materials which include conducting, semiconducting and even insulating samples.[1,2] In addition to surface characterization, AFM has been employed to modify the substrate surfaces locally either by application of force or bias.[3] In the force assisted AFM nanolithography, the force applied on the tip is larger than for normal AFM imaging which may bring local physical modifications to surfaces via elastic or plastic deformations. Mechanical indentation, scratching, plowing, and nanomanipulation come under the category of force assisted AFM nanolithography where the tip-sample interactions are of mechanical in nature.[4,5] Dip-pen nanolithography (DPN) is a direct write lithographic technique in which an AFM tip coated with the functional molecules which get transported to the substrate surface aided by the water meniscus formed at the tip-sample interface.[6] DPN has been used extensively to pattern a wide variety of inks such as small organic molecules, polymers, bio-molecules, colloids and metal ions onto surfaces with nanoscale resolution.[6–8] The water meniscus which forms at the tip-sample interface has also been employed as an electrolyte to set up a nanoelectrochemical cell under a biased AFM tip. The applied voltage bias of few volts would generate an electric field of 10^9–10^{10} V/m which induces the ionization of water molecules, leading to the generation of oxidative species (OH^-, O^-) which cause the oxidation of material surfaces locally, known as local anodic oxidation (LAO).[9]

LAO has been employed to fabricate nanoscale oxide features on various materials which include metals, semiconductors and even sometime insulators.[3] In the case of polymeric films, the intense electric fields can cause local ablation due to joule heating while mild electric field

[a]Email: narendra@jncasr.ac.in

 © Author(s) 2013

All article content, except where otherwise noted, is licensed under a Creative Commons Attribution 3.0 Unported license. See: http://creativecommons.org/licenses/by/3.0/
Downloaded to IP: 129.21.35.191 On: Sun, 21 Dec 2014 15:36:59

brings in electrochemical or electrostatic modifications.[10–12] Nanoscale explosion and shock wave propagation have also been observed in case of polymers and semiconductor surfaces under higher humidity and bias conditions.[13–15] Besides the above mentioned local chemical modifications, AFM bias lithography has also been employed to write charge patterns on the electret films,[16] polymers,[17] fluorocarbon films[18] and recently $LaAlO_3/SrTiO_3$ interfaces.[19] Thus, AFM bias lithography has become an effective tool to cause various kinds of local modifications depending on the material surface and operating conditions. Here, in this report, AFM bias lithography has been employed to cause various kinds of electrochemical and physical modifications on a single surface namely, carbonaceous platforms fabricated by electron beam induced deposition.

The carbonaceous platforms have been fabricated by the exposure of focused electron beam on a surface in presence of abundant residual hydrocarbons of the scanning electron microscope (SEM) vacuum chamber or by supplying pump oil as hydrocarbon source.[20,21] These carbonaceous deposits were employed as etch masks for micromachining[22] and local dielectric for CNT circuits[20,21] due to their chemical inertness and electrically insulating nature. EBICD was also utilized as a nano-solder material to improve the mechanical and electrical properties of CNT-electrode interfaces.[23,24] However, the unique surface properties of EBICD surface have not been explored by means of local probe techniques. Here, in this report, the unique and diverse surface properties of EBICD have been investigated by employing AFM bias lithography under different operating conditions such as mode of operation, tip bias polarity and humidity. Positively biased AFM tip in the tapping mode under moderate humidity conditions (40-45%) could nucleate attoliter water on the EBICD surface, reported in our previous studies.[25] Besides the water condensation, in the present study, the possibility of local chemical and physical modifications on the EBICD surface such as anodic oxidation, electrochemical etching and charge writing have been studied. Tunable AFM bias lithography on EBICD surface has been achieved by a careful selection of the operating conditions such as humidity, mode of operation and tip bias polarity. Lithography in the contact mode with a negative tip bias resulted in the electrochemical modifications such as anodic oxidation and etching of the EBICD under moderate (45%) and higher (60%) humidity conditions respectively. Reversible charge patterns have been created on these EBICD surfaces under low (30%) humidity conditions in contact mode.

II. EXPERIMENTAL

Silicon substrates of 1×1 cm^2 dimensions are cut from the n-type Si wafer ($\rho = 4$–7 Ω.cm) followed by cleaning through sonication in acetone, ethanol and double distilled water for 5 minutes. Electron beam induced carbonaceous deposition was performed using a Nova NanoSEM 600 FESEM system (FEI Company) in environmental mode making use of the residual hydrocarbons present in the chamber.[25] The pole piece was mounted with a low vacuum detector (LVD), the chamber was evacuated and subsequently backfilled with water vapor to a pressure of 0.4 Torr. Selected regions on the substrate were exposed to e-beam dosages of 0.7–2.5 C cm^{-2} at 10 kV in the patterning mode at a working distance of 3–4 mm. Large area carbonaceous depositions are created by raster scanning of the e-beam in TV mode. Carbonaceous deposit over a large area on Si substrate was used for X-ray photoelectron Spectroscopy (XPS) analysis. XPS measurements have been carried out using Omicron SPHERA spectrometer with non-monochromatic AlK_α X-rays (E = 1486.6 eV). AFM imaging and bias lithography were performed at room temperature employing a Dimension 3100 SPM with a NS-IV controller (Veeco, USA). Both intermittent contact (dynamic AFM) and direct contact scanning modes were used. Metalized Pt/Ir coated Si cantilevers with a nominal spring constant of 2.2 N/m and resonance frequency of 75 kHz (Veeco Model, SCM-PIT) were used for tapping mode AFM. For contact mode operation, Pt/Ir coated Si cantilevers (Veeco Model SCM-PIC) with a nominal spring constant of 0.2 N/m and resonance frequency of 16 kHz were used. Typically, a set point force in the range 6–8 nN was used during contact mode lithography. In intermittent contact scans, the free amplitude cantilever oscillation was set to 30–40 nm when the tip was far from the substrate. Tapping mode imaging and lithography were performed with a set point amplitude ratio of 50–60%. A bias voltage could be applied to the metalized AFM tips using the AFM controller electronics and a controllable tip biases ranging from −10 to +10 V, scan speed of 0.5–1 μm/s were used during lithography keeping the substrate grounded. All the experiments

All article content, except where otherwise noted, is licensed under a Creative Commons Attribution 3.0 Unported license. See: http://creativecommons.org/licenses/by/3.0/
Downloaded to IP: 129.21.35.191 On: Sun, 21 Dec 2014 15:36:59

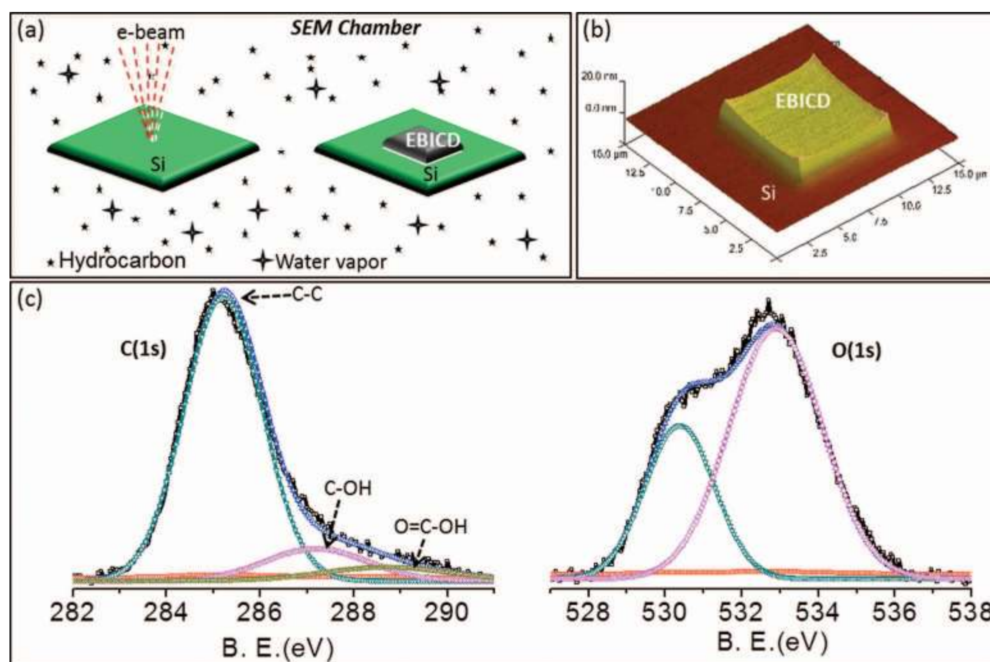

FIG. 1. (a) Schematic illustration of the process of electron beam induced carbonaceous deposition in environmental scanning electron microscope. (b) The 3-D AFM image of the carbonaceous platform on Si surface. (c) C1s and O1s core-level X-ray photoelectron spectra of the EBICD on Si. Gaussian peak fittings are employed after appropriate background correction.

were carried out in ambient conditions under varied relative humidity of 30–60%. Electrostatic force microscopy (EFM) was performed using a biased conducting tip coated with a 30 nm layer of Pt/Ir evaporated on top of a thin 3 nm Cr adhesion layer. The electrostatic force was detected as a phase shift in the cantilever response with respect to the dither piezo drive signal as measured after performing a topographic line scan and then lifting the tip by an additional height of 120 nm.

III. RESULTS AND DISCUSSION

The schematic illustration of electron beam induced carbonaceous deposition on a Si substrate is shown in Fig. 1(a). The residual hydrocarbons abundant in the environmental SEM along with the water molecules get adsorbed onto the loaded substrate. The exposure of focused electron beam triggers a set of complex reactions involving hydrocarbons leading to the formation of solid carbonaceous deposits on the substrate.[20–24] The carbonaceous deposition on the Si (shown in Fig. 1(b)) substrate is created with an e-dosage of 2.5 C cm^{-2} at 10 kV beam energy. The corresponding 3-D AFM image of the carbonaceous deposit with a nominal thickness of ∼10 nm is shown in Fig. 1(b). The chemical composition of the EBICD was investigated by X-ray photoelectron spectroscopy (XPS) analysis. Figure 1(c) shows the core level spectra of the large area carbonaceous deposit on the Si substrate. The C1s spectrum shows the main peak at 285.2 eV (C-C sp^3) and additional peaks at 287.2 and 288.7 eV corresponding to C=O and O=C-OH groups.[26] Similarly, O1s contains two peaks at 530.4 and 532.9 eV due to O=C, O=C-OH and C-OH groups respectively. The atomic ratio of carbon to oxygen was estimated to be 2.7:1. Thus, the electron beam stitches the residual hydrocarbons in the form of functionalized carbonaceous species on a given substrate where the approximate carbon to oxygen ratio is found to be 75:25. Certainly, carbon to oxygen ratio depends on the pressure of water used in the chamber during the process of electron beam induced carbonaceous deposition (EBICD). Without the introduction of water vapor when the chamber pressure is 10^{-6} Torr (high vacuum grade), carbon to oxygen ratio in EBICD is found to be 85:15. Thus, carbon to oxygen ratio in EBICD depends primarily on the amount of water vapor present in the vacuum chamber. The additional ionic current contributed from the water moisture of

All article content, except where otherwise noted, is licensed under a Creative Commons Attribution 3.0 Unported license. See: http://creativecommons.org/licenses/by/3.0/
Downloaded to IP: 129.21.35.191 On: Sun, 21 Dec 2014 15:36:59

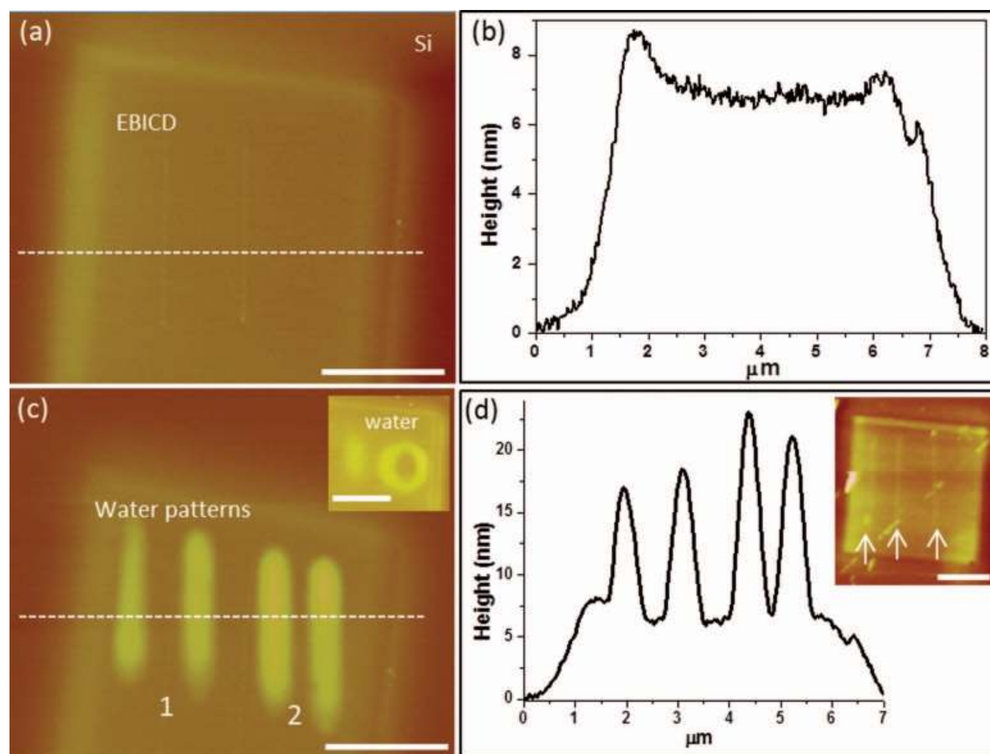

FIG. 2. (a) AFM topography and (b) z-profile of the EBICD platform on Si. (c) Topography of the nucleated water patterns (tip voltages of 4 and 5 V are used for the sets 1 and 2, respectively), inset shows the circular water pattern on the EBICD surface. (d) z-profile for the nucleated water features (8–15 nm) at relative humidity of 40–45%. Inset shows the meek oxide features on the EBICD surface, produced with a tip bias of −10 V in tapping mode at a relative humidity of 40–45%. Oxide features are indicated with arrows. Scale bar, 2 μm.

the environmental mode (chamber pressure ∼0.4 Torr) results in the thicker carbonaceous platforms compared to high vacuum mode (chamber pressure $\sim 10^{-6}$ Torr).[27]

AFM bias lithography was performed on the EBICD platforms in different modes with varied tip bias and polarity under controlled humidity conditions. Initially, the bias lithography was performed in tapping mode with a positive tip bias at humidity of 40–45%. Figure 2(a) shows the AFM topography of the EBICD platform on Si and its thickness is found to be ∼8 nm (see Fig. 2(b)). Lithography using positive tip biases in the tapping mode resulted in the formation of raised features (see Fig. 2(c)). The raised features of height ∼8 and 15 nm were created using tip bias voltages of 4 and 5 V (sets 1 and 2) respectively at a scan speed of 1 μm/s (see Fig. 2(d)). These raised features, attributed to the nucleated water patterns which eventually undergoing evaporation, leading to the decrease in height of the water features with time (vide infra). It is essentially an electro-condensation process induced by a positively biased AFM tip in tapping mode under moderate humid conditions (RH, 40–45%).[25] While the negatively biased AFM tip under same conditions could not assist the nucleation of water on the EBICD surface but resulted in the meek oxide features which were found to be permanent with time (see inset of Fig. 2(d)).

Time dependent behavior of the raised features was monitored in successive tapping mode AFM images (see Fig. 3). Interestingly, the raised patterns disappear slowly with time as evident from the images in Fig. 3 (see Fig. 3(a) to 3(d)). This indicates that there is no chemical modification to the carbonaceous platform during the positive tip bias tapping mode lithography; rather temporary physical changes such as nucleation of water patterns on the surface which eventually underog evaporation with time. The evaporation rate is found to be 2 aL/min., exhibiting very slow evaporation kinetics of electrocondensed water patterns.[25]

In order to study the influence of mode of operation, AFM bias lithography was performed in contact mode. Figure 4(a) shows the AFM topography of the EBICD (thickness ∼10 nm) on the

All article content, except where otherwise noted, is licensed under a Creative Commons Attribution 3.0 Unported license. See: http://creativecommons.org/licenses/by/3.0/
Downloaded to IP: 129.21.35.191 On: Sun, 21 Dec 2014 15:36:59

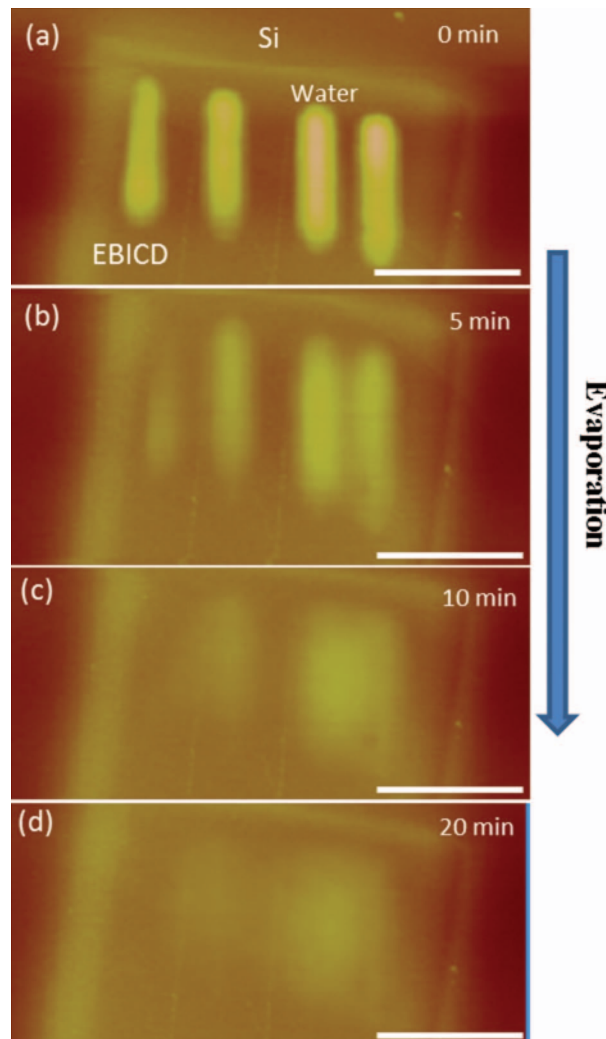

FIG. 3. Evaporation of the condensed water patterns on EBICD. (a)–(d) AFM topography showing temporal behavior of the water patterns, tapping mode images recorded at different times are shown. Scale bar, 2 μm.

Si substrate. Lithography was performed by drawing lines from Si to the EBICD using negatively biased AFM tip (−10 V) at a relative humidity of 45%. At these conditions, the biased AFM tip initiates local anodic oxidation of both Si and EBICD, which can be seen as raised features which remained indefinitely (see Fig. 4(b)).[9,28] The inset shows a zoom-in-view of the grid pattern of oxide lines on the EBICD surface. The typical height of these features is 1.5–2 nm as determined from the corresponding z-profile (see Fig. 4(c)). Further, lithography was performed in contact mode with a tip bias of −10 V at higher relative humidity of 60%. Lithography was performed on the set of EBICD platforms (thickness ∼5 nm) on Si is shown in Fig. 4(d). After performing lithography, almost the entire region underwent modification (see Fig. 4(e)).

This is due to parallel spreading of oxidative species on the substrate surface under high humidity conditions.[13,14] After performing the lithography in the contact mode (tip bias of −10 V) under high humidity conditions (60%), the spatial distribution of oxidative species leading to the transient shockwave propagation in the surrounding regions where the lateral spread of the oxidative species etch away the surrounding carbonaceous platforms (shown with arrows in the inset of Fig. 4(f)). AFM z-profile analysis in Fig. 4(f) shows that ∼2 nm of the EBICD got etched away during this process as the oxidative species transformed solid carbon into volatile CO and CO_2.[28] The propagation of the shock waves can spread the oxidative species to a lateral distance of several

All article content, except where otherwise noted, is licensed under a Creative Commons Attribution 3.0 Unported license. See: http://creativecommons.org/licenses/by/3.0/
Downloaded to IP: 129.21.35.191 On: Sun, 21 Dec 2014 15:36:59

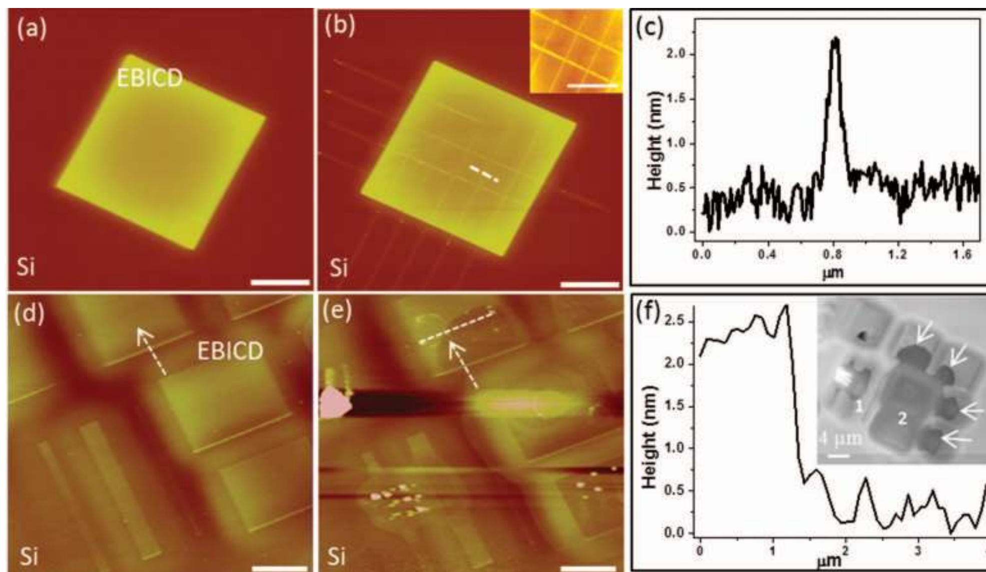

FIG. 4. Electrochemical modifications on Si and EBICD surfaces with a negatively biased AFM tip (−10 V) in contact mode. (a) AFM topography of the EBICD on Si. (b) oxide patterns in the form of lines on the Si and EBICD surfaces (RH = 40–45%). Inset shows the grid pattern of oxide features on the EBICD surface. (c) z-profile for the oxide feature of the EBICD. AFM topography of the (d) EBICD platforms and (e) electrochemical etching of EBICD under high humidity (RH = 60%) conditions. Scale bar, 3 μm. (f) AFM z-profile for the etched part of the EBICD platform with respect to the unmodified region (dotted line in the (e)). Arrows in the (d) and (e) show the regions before and after electrochemical etching event respectively. Inset shows SEM image of etched EBICD platforms due to lateral spreading of oxidative species.

μms generating oxide structures on the Si surface.[13] This behavior is also observed in the case of polymer films and semiconductor surfaces under higher humidity conditions, where nanoexplosion under the tip apex assisted by shock wave propagation leading to the formation of center cone and outer ring-like structures.[13–15]

AFM bias lithography has been performed on the EBICD surface under lower humidity conditions (RH = 30%) in the contact mode. Tip biases of +6 and −10 V are applied to write the lines on the top and bottom EBICD platforms respectively. No appreciable changes in the topography of the EBICD surfaces were seen before and after writing with the given tip biases (see Figs. 5(a) and 5(b)). Electrostatic force microscopy (EFM) was employed to examine whether there exist any charge patterns which could not been seen in topography. During EFM studies, dc bias voltage on the tip was employed in the lift scan mode in order to map the electrostatic force gradients which are directly proportional to the observed EFM phase shifts. In this technique, as there is no AC component of voltage employed, hence no AC modulation frequency used during recording of EFM technique. EFM technique involves applying dc voltage on tip or sample and there are no frequency terms (ω, 2ω) during recording of EFM image. To determine the sign of these surface charges, EFM phase images were recorded with V_{read} of −3 and +3 V, both at a lift scan height of 120 nm. In EFM, attractive and repulsive force gradients result in the negative and positive phase shifts which give darker and brighter contrasts respectively. The three lines written with a V_{write} of +6 V on the top EBICD platform showed bright and dark contrasts for V_{read} of −3 and +3 V respectively. On the other hand, the lines written with −10 V on the bottom EBICD platform showed dark and bright contrasts for V_{read} of −3 and +3 V respectively (see Figs. 5(c)–5(f)). This indicates that the writing with a positive tip bias results in the negative surface charges and reverses for the negative tip bias writing. This observation was further confirmed by drawing lines with V_{write} of −10 V on the top EBICD platform without rewriting on the bottom. Now the top and bottom platforms showed similar contrasts for the lines, indicating the possibility of reversible charge writing depending on the sign of $V_{write.}$

Further, circular charge patterns were made with +6 V and −10 V on top and bottom EBICD paltforms followed by imaging them using EFM technique (see Figs. 6(a) and 6(b)). Thus, under

All article content, except where otherwise noted, is licensed under a Creative Commons Attribution 3.0 Unported license. See: http://creativecommons.org/licenses/by/3.0/
Downloaded to IP: 129.21.35.191 On: Sun, 21 Dec 2014 15:36:59

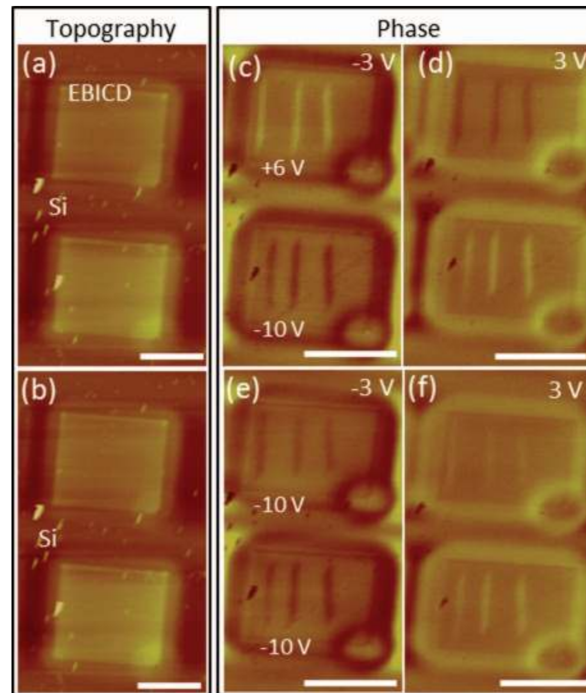

FIG. 5. (a) and (b) AFM topography of the EBICD platforms before and after charge patterning respectively. EFM phase images after writing three lines at V_{write} of +6 V (top), −10 V (bottom), read with V_{read}, −3 V (c), and +3 V (d), lift scan height of 120 nm. EFM phase images with V_{read} of (e) −3 V and (f) 3 V after rewriting with a tip bias of −10 V on same patterns of the top EBICD platform. Scale bar, 3 μm.

low humidity conditions (∼30%), it is possible to write the charge patterns on EBICD surface in a reversible manner. This phenomenon can be explained by the water-cycle mechanism[29] in which the electrochemical reactions are not favorable on these EBICD platforms rather only physical processes such as charge patterning is possible at low humidity conditions. As charge patterning involves no changes in the topography, it can only be detected either through EFM or Kelvin probe force microscopy (KPFM) imaging. Although, KPFM is a direct method for estimating the local surface potentials quantitatively, its spatial resolution is relatively poor due to the long range property of electrostatic forces. While EFM phase method is based on measuring electrostatic force gradients, resolution is much better compared to KPFM technique. Hence, EFM phase and KPFM techniques could be helpful in studying the local charge patterns with high resolution in a quantitative manner where topography imaging would be of no use in estimating charge patterns. It is known that the negative and positive tip biases drive the OH^- and H^+ ions respectively towards the substrate surface, resulting in charge deposition on the EBICD surface. Under low humidity conditions, the number of the oxidative ions are low enough not causing the local chemical modification but only resulting in the physical modifications such as charge writing through deposition of ions.

A summary of the AFM bias lithography on the EBICD surface is presented in Fig. 7. The surface of EBICD could nucleate the attoliter water under a positively biased AFM tip in tapping mode at a moderate humidity (45%). As the humidity is decreased to 30%, the formation of reversible charge patterns are observed depending on the tip bias polarity guided by the water-cycle mechanism.[28] These modifications are of electrophysical in origin which do not involve any chemical modifications to the EBICD surface. AFM bias lithography in contact mode with a negatively biased AFM tip has induced local anodic oxidation of the EBICD surface under moderate humidity (45%). Further, increase in the humidity up to 60% resulted in the lateral spreading of oxidative species (which is known in the literature as shock wave propagation) causing the electrochemical etching of the EBICD surfaces over microns range.

All article content, except where otherwise noted, is licensed under a Creative Commons Attribution 3.0 Unported license. See: http://creativecommons.org/licenses/by/3.0/
Downloaded to IP: 129.21.35.191 On: Sun, 21 Dec 2014 15:36:59

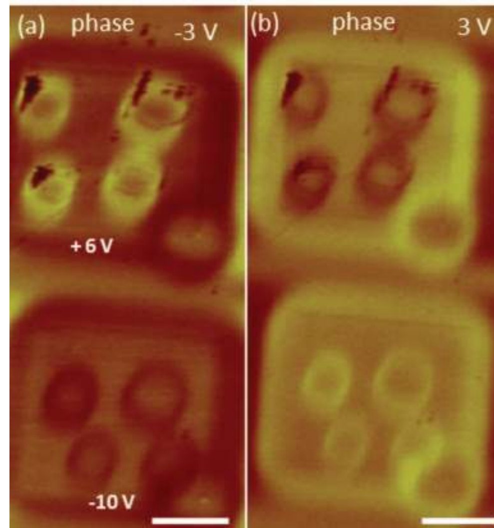

FIG. 6. EFM phase images after writing circular charge patterns with V_{write} of +6 V (top), −10 V (bottom), read with V_{read}, −3 V (a), and +3 V (b), lift scan height of 120 nm. Scale bar, 2 μm.

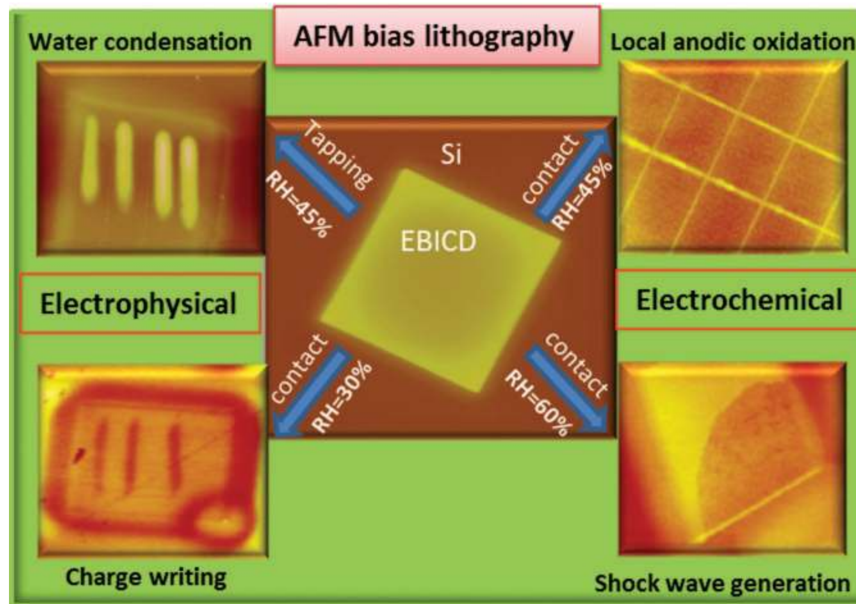

FIG. 7. AFM bias lithography on the EBICD surface with possible electrophysical modifications such as water condensation and charge patterning and the electrochemical modifications such as local anodic oxidation and etching depending on the mode of operation, tip bias polarity and relative humidity.

The novel surface functionality of the EBICD surface is responsible for the tunable local modifications according to the operating conditions adopted. The e-beam is inducing the complex reactions of residual hydrocarbons along with the moisture leading to the formation of stitched carbonaceous patterns. The carbon to oxygen ratio of the carbonaceous deposits is found to be 75:25, determined through XPS analysis. AFM as a local probe technique has been employed to exploit the unique surface functionality of the EBICD surface. Firstly, EBICD has been employed as a suitable platform for nucleating the water patterns and their stability under ambient conditions. This can be explained by the polarization surface functional groups under the electric field from the AFM tip followed by subsequent electrostatic clamping of water molecules leading to the nucleated

All article content, except where otherwise noted, is licensed under a Creative Commons Attribution 3.0 Unported license. See: http://creativecommons.org/licenses/by/3.0/
Downloaded to IP: 129.21.35.191 On: Sun, 21 Dec 2014 15:36:59

water features. The relaxation of polarized functional groups with time causing detachment of water molecules leading to evaporation. Thus, the reversible polarization of surface functional groups has allowed in studying the nature of water condensation under different tip bias conditions during tapping mode of operation. On the other hand, local electrochemical modifications of the EBICD surface were obtained using a negative tip bias in the contact mode. At moderate humidity, the oxidation of the EBICD surface has been observed while at higher humidity the spreading of the oxidative species via shock wave propagation causing the electrochemical etching of the EBICD surfaces over large areas. Apart from these permanent chemical modifications, the charge patterns on the EBICD surfaces have been written under low humidity in contact mode. The charge patterns have been reversibly changed according to the polarity of tip bias. As there is no change in the topography, the written charge patterns have been imaged through EFM. Thus, the electrophysical processes such as water condensation, charge patterning and electrochemical modifications such as anodic oxidation and etching of the EBICD surfaces have been realized by choosing the appropriate operating conditions.

IV. CONCLUSIONS

In summary, a set of conditions for electrophysical and chemical modifications on a dielectric EBICD surface have been arrived by employing a biased AFM tip under different humidity conditions and mode of operation. The carbonaceous platforms on Si were created by the electron beam induced deposition using residual hydrocarbons along with water vapor at 0.4 Torr. The carbonaceous deposits contain functional groups such as carbonyl, carboxyl and hydroxyl etc. AFM bias lithography was performed by employing different conditions such as mode of operation, polarity of the tip bias and relative humidity. Humidity conditions of 40–45% favor the local anodic oxidation in either contact or tapping modes under a negative tip bias. Further, higher humidity conditions (∼60%) cause the spatial distribution of oxidative species due to shock wave generation. Under low humidity conditions (∼30%), reversible charge patterns have been created depending on the tip bias polarity. Exclusively, positive tip voltages in the tapping mode at humidity of 40–45% favor the condensation of water on the carbonaceous platforms.

ACKNOWLEDGMENTS

The author thanks Professor G. U. Kulkarni for his encouragement, suggestions and guidance in writing up this manuscript. NK thank Professor C N R Rao, FRS for his encouragement. NK thank Dr. Vijay and Dr. Basava Raja for their help in various aspects. Support from the Department of Science and Technology, Government of India is gratefully acknowledged. NK acknowledges CSIR for funding and Veeco India Nanotechnology Laboratory at JNCASR for the AFM facility.

[1] G. Binnig, C. F. Quate, and C. Gerber, Phys. Rev. Lett. **56**, 930 (1986).
[2] D. Bonnell, *Scanning Probe Microscopy and Spectroscopy*; Ed.; (Wiley-VCH, New York, 2000).
[3] X. N. Xie, H. J. Chung, C. H. Sow, and A. T. S. Wee, Mater. Sci. Eng. R **54**, 1 (2006).
[4] B. Cappella and H. Sturm, J. Appl. Phys. **91**, 506 (2002).
[5] Y. Sugimoto, M. Abe, S. Hirayama, N. Oyabu, Ó. Custance, and S. Morita, Nat. Mater. **4**, 156 (2005).
[6] K. Salaita, Y. Wang, and C. A. Mirkin, Nat. Nanotech. **2**, 145 (2007).
[7] D. S. Ginger, H. Zhang, and C. A. Mirkin, Angew. Chem., Int. Ed. **43**, 30 (2003).
[8] R. D. Piner, J. Zhu, F. Xu, S. Hong, and C. A. Mirkin, Science **283**, 661 (1999).
[9] R. Garcia, R. V. Martinez, and J. Martinez, Chem. Soc. Rev. **35**, 29 (2006).
[10] S. F. Lyuksyutov, R. A. Vaia, P. B. Paramonov, S. Juhl, L. Waterhouse, R. M. Ralich, G. Sigalov, and E. Sancaktar, Nat. Mater. **2**, 468 (2003).
[11] T. Vijaykumar and G. U. Kulkarni, Nanotechnol. **18**, 445303 (2007).
[12] M. A. Reagan, D. Kashyn, S. Juhl, R. A. Vaia, and S. F. Lyuksyutov, Appl. Phys. Lett. **93**, 033109 (2008).
[13] X. N. Xie, H. J. Chung, Z. J. Liu, S. -W. Yang, C. H. Sow, and A. T. S. Wee, Adv. Mater. **19**, 2618 (2007).
[14] X. N. Xie, H. J. Chung, C. H. Sow, K. Adamiak, and A. T. S. Wee, J. Am. Chem. Soc. **127**, 15562 (2005).
[15] X. N. Xie, M. Deng, H. Xu, S. W. Yang, D. C. Qi, X. Y. Gao, H. J. Chung, C. H. Sow, V. B. C. Tan, and A. T. S. Wee, J. Am. Chem. Soc. **128**, 2738 (2006).
[16] P. Mesquida and A. Stemmer, Adv. Mater. **13**, 1395 (2001).
[17] L. Ressier and V. L. Nader, Nanotechnol. **19**, 135301 (2008).
[18] P. Mesquida, H. F. Knapp, and A. Stemmer, Surf. Interface Anal. **33**, 159 (2002).

All article content, except where otherwise noted, is licensed under a Creative Commons Attribution 3.0 Unported license. See: http://creativecommons.org/licenses/by/3.0/
Downloaded to IP: 129.21.35.191 On: Sun, 21 Dec 2014 15:36:59

[19] Y. Xie, C. Bell, T. Yajima, Y. Hikita, and H. Y. Hwang, Nano Lett. **10**, 2588 (2010).
[20] K. Narendra, T. Vijay kumar, and G. U. Kulkarni, J. NanoSci. Nanotechnol. **11**, 1025 (2011).
[21] N. Miura, H. Ishii, J. Shirakashi, A. Yamada, and M. Konagai, Appl. Surf. Sci. **113–114**, 269 (1997).
[22] N. Morita, N. Kawasegi, and K. Ooi, Nanotechnol. **19**, 155302 (2008).
[23] A. Bachtold, M. Henny, C. Terrier, C. Strunk, C. Schönenberger, J. P. Salvetat, J. M. Bonard, and L. Forró, Appl. Phys. Lett. **73**, 274 (1998).
[24] M.-F. Yu, O. Lourie, M. J. Dyer, K. Moloni, T. F. Kelly, and R. S. Ruoff, Science **287**, 637 (2000).
[25] N. Kurra, A. Scott, and G. U. Kulkarni, Nano Res. **3**, 307 (2010).
[26] S. Yumitori, J. Mater. Sci. **35**, 139 (2000).
[27] N. Kurra, V. S. Bhadram, C. Narayana, and G. U. Kulkarni, ACS Appl. Mater. Interfaces **4**, 1030 (2012).
[28] A. Avramescu, A. Ueta, K. Uesugi, and I. Suemune, Appl. Phys. Lett. **72**, 716 (1998).
[29] F. Bi, D. F. Bogorin, C. Cen, C. W. Bark, J.-W. Park, C.-B. Eom, and J. Levy, Appl. Phys. Lett. **97**, 173110 (2010).

All article content, except where otherwise noted, is licensed under a Creative Commons Attribution 3.0 Unported license. See: http://creativecommons.org/licenses/by/3.0/
Downloaded to IP: 129.21.35.191 On: Sun, 21 Dec 2014 15:36:59